CHARACTERISATION OF INDUSTRIAL-SCALE REMOTE PECVD SiN DEPOSITIONS

Saul Winderbaum[1], Anthony J. Leo[2], Stephen P. Shea, Timothy D. Koval[3], Bikash Kumar[4]
1. Shamash Australia Pty Ltd, 2. bp solar Australia, 3. bp solar USA, 4. Tata bp solar India

ABSTRACT

Remote PECVD SiN deposition parameters have been optimised for a fired-through metallization process on multicrystalline silicon solar cells.

The best pressure, gas ratio and deposition temperature resulted in cell efficiencies of up to 14.3% when used with a 30 Ohm/square emitter and above 15% for 40 Ohm/square diffusion.

Fourier transform infrared spectroscopy revealed that, during firing, the films lost a significant proportion of their hydrogen content, providing good bulk and surface passivation. In all cases the refractive index was reduced by approximately 1% during firing.

The parameter space that gives optimal conditions for the lighter emitter coincides with a region in which the refractive index can be varied, resulting in greater process flexibility.

1. INTRODUCTION

Firing the front metal contacts of multicrystalline silicon solar cells through a plasma-enhanced chemical vapour deposited silicon nitride (PECVD SiN) film offers many advantages.

As well as providing bulk hydrogenation and surface passivation, it allows simultaneous firing of front and back contacts and improved yield. In addition, as with any screen printed fire through scheme it offers protection for the emitter surface further reducing yield losses through less shunt failures.

In this work, SiN deposition parameters (temperature, pressure and gas ratios) have been optimised to maximise multicrystalline silicon cell performance after firing through.

The optical properties of the films have been characterised by ellipsometry, and their chemical composition analysed using Fourier Transform Infrared Spectroscopy (FTIR), before and after firing.

2. EXPERIMENTAL SET-UP

The deposition system used is an in-line, quasi-continuous, remote PECVD system [1].

The system is modular, consisting of three main chambers, separated by gate valves, load, and unload lock chambers and a process chamber.

The process chamber can be functionally separated into three areas, heating channel, where substrates and carriers are stabilised at their deposition temperature, a cooling area, after deposition, that allows for the carrier and cells to cool down before exiting the system, and the deposition area, in which, four linear plasma sources excite the reactive gases, in this case SiH_4 and NH_3 at a frequency of 2.45 GHz.

The system uses an Edwards EH4200/GV600 pump stack as the main process-pumping unit for the three chambers, although a Turbo molecular pump is available for pumping to UHV levels when and if that is necessary.

Process pressure is controlled independently of gas flows via a VAT controller valve or speed control system for the pumps themselves.

Deposition rate in this system varies between 80 to 100 nm/min depending on processing parameters, which in turn, at an availability rate of 75% means a throughput between 24 to 30 MW/year.

A picture of such a system is presented in Figure 1

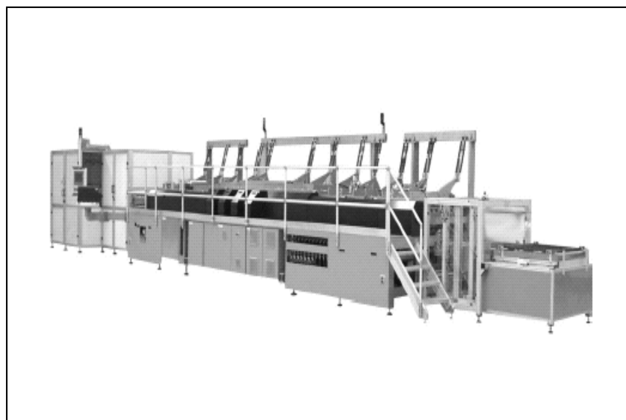

Figure 1.In-line PECVD system

In the first trial, using a design of experiments methodology, nine combinations of deposition parameters were used based on a central composite design [2,3], with the process pressures ranging from 0.13 to 0.27 mbar, temperature from 340 to 410°C, and the ammonia/silane gas ratio from 2.2 to 3.6.

A relatively narrow range of refractive index was maintained in order to null optical differences that could otherwise skew the results.

This was achieved by altering the gas ratio at each temperature and pressure combination, meaning that gas ratio was not a truly free parameter in this optimisation.

In a second trial, the gas ratio was varied directly, as was the pressure, while maintaining the temperature at 400°C.

Two different diffusion conditions were included in this second trial to test the sensitivity of the process to the emitter profile.

For both trials, 10 cross-matched wafers from a single brick were processed for each condition.

In both trials, the performance of the process was evaluated in a twofold way, first by measuring the average V_{OC} for the process conditions and secondly measuring the improvement in the J_{SC} and V_{OC} when compared to a TiO_2 process in which the metallization is not fired-through the coating. In this way differences in FF derived from other factors during the metallisation can be isolated.

3. RESULTS

3.1. Results of first trial

In Table I it can be seen that process DOE1_6 gave the best improvement in cell performance, measured by the percentage improvement of $J_{SC}*V_{OC}$ and by V_{OC}, although all processes led to significant improvements.

Deposition	Av. V_{OC} (mV)	$J_{SC}*V_{OC}$ % gain
DOE 1_1	599.0	7.6
DOE 1_2	595.7	6.9
DOE 1_3	597.7	6.0
DOE 1_4	596.9	6.9
DOE 1_5	598.0	7.1
DOE 1_6	600.5	8.3
DOE 1_7	597.0	7.7
DOE 1_8	596.6	7.4
DOE 1_9	597.0	7.7

Table I. First trial average V_{OC} cell results, and $J_{SC}*V_{OC}$ gain in %

This is consistent with previous work, which has shown that optimum passivation arises when the temperature is kept high and the process pressure low.

For each one of the deposition conditions in the first trial, a CZ single crystal silicon polished wafer was run to measure the refractive index and thickness of the deposited layer.

A reduction in refractive index of about 1% in value after treating the CZ wafers with a metallisation firing profile was observed for all deposition conditions, this data is presented in Table II

Deposition	R.I. Before Firing	R.I. After Firing	R.I. % Change
DOE 1_1	2.037	2.018	-0.9
DOE 1_2	2.037	2.014	-1.1
DOE 1_3	2.042	2.019	-1.1
DOE 1_4	2.051	2.028	-1.1
DOE 1_5	2.040	2.013	-1.3
DOE 1_6	2.021	1.999	-1.1
DOE 1_7	2.030	2.007	-1.1
DOE 1_8	2.060	2.036	-1.2
DOE 1_9	2.047	2.022	-1.2

Table II. Deposition parameters, refractive indices before and after firing,

Film thickness remained unchanged after the wafers went through the metallisation firing profile. This was contrary to our initial expectation.

However the hydrogen-bonding scheme was changed significantly, as shown on Table III. For all deposition conditions the N-H bond concentration decreased after firing, while the Si-H bond concentration increased in all but two cases. In all cases, both the atomic % ratio N-H: Si-H in the film and the total amount of Hydrogen decreased after firing. The relative decrease in total Hydrogen ranged between from 3.5% and 16.8 %, as shown in the table.

Another important point to note at this stage is that the maximum change for the total Hydrogen after firing occurred for those deposition conditions in which the change in Si-H % was lowest, DOE1_3, DOE1_5. [3]

Deposition	%Change [N-H] After firing	%Change [Si-H] After firing	%Change Total H After firing
DOE 1_1	-30.8	27.9	-5.2
DOE 1_2	-21.8	10.3	-6.8
DOE 1_3	-32.2	-1.1	-15.6*
DOE 1_4	-37.8	12.7	-8.4
DOE 1_5	-36.6	-1.8	-16.8*
DOE 1_6	-26.2	1.9	-11.7
DOE 1_7	-32.3	15.3	-6.5
DOE 1_8	-32.1	6.9	-9.0
DOE 1_9	-23.2	11.8	-3.5

Table III Deposition parameters and changes in N-H and Si-H bond concentrations and total H concentration within the SiN film after firing

Table IV gives the electrical parameters for the best multicrystalline cell from process DOE1_6, which had efficiency of 14.36% and for the best cell on the second trial, with an efficiency of 15.01%.

#	Eff (%)	P_{max} (W)	I_{SC} (A)	V_{OC} (mV)	FF
1	14.36	2.24	4.93	601	75.7
2	15.01	2.34	4.96	608	77.7

Table IV. Cell parameters for the best multicrystalline silicon cell from trial 1, and from trial 2, at R_{sheet}=40Ω/sqaure.

3.2. Results of second trial

From the second trial, the refractive index and finished cell parameters were both measured as a function of gas ratio and pressure.

Interestingly, the region of maximum efficiency coincides with a region of almost constant refractive index.

This results in some flexibility in choosing the processing parameters, such as deposition pressure and gas ratio to obtain this optimal refractive index while retaining the best electronic properties.

However for a lighter emitter, in this case, a 40Ohm/square, the region of optimal processing

conditions is shifted to a zone in which gas ratio is smaller and pressure higher.

This fact is an example of the interaction dynamics between diffusion profiles and optimum PECVD SiN deposition conditions.

The best multicrystalline cell from this lighter emitter batch reached 15%, as shown in Table IV.

Typical Quantum efficiency and IV curves for cells made using the process developed during this work are presented below in Figures 2 and 3.

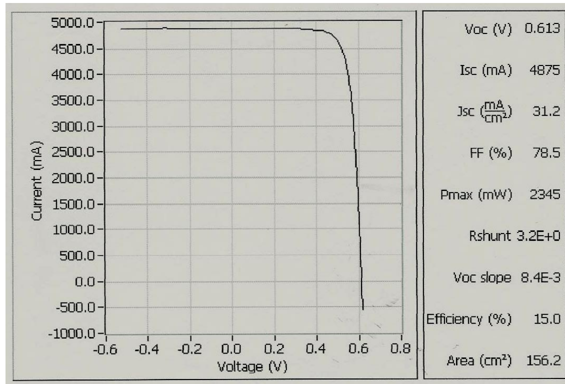

Figure 2. Typical IV curve

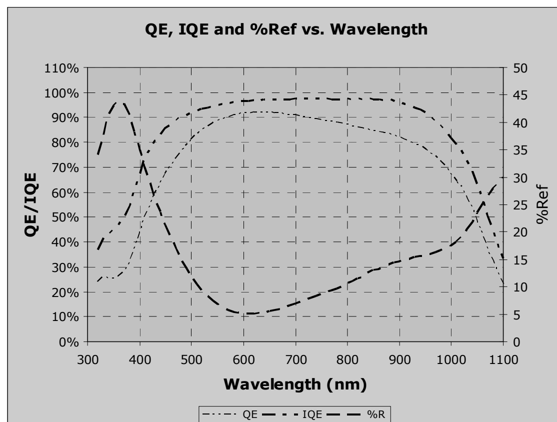

Figure 3. Typical EQE and IQE curves for the process developed in this paper

A comparison between the internal quantum efficiency for matched cells between the two emitters with the same Silicon Nitride process is presented in Figure 4.

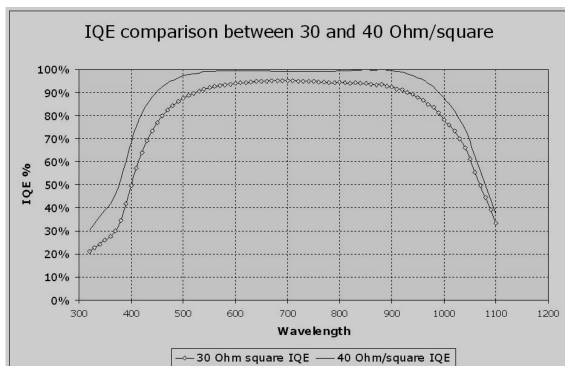

Figure 4 IQE curve comparison for 30 and 40 Ohm/square emitter

Additional process optimization has produced multicrystalline cells with V_{OC}=615mV and J_{SC}>5A. Improvements have also been made in cells encapsulated performance, as shown in Figure 5, resulting in the best match of process conditions to the final module result.

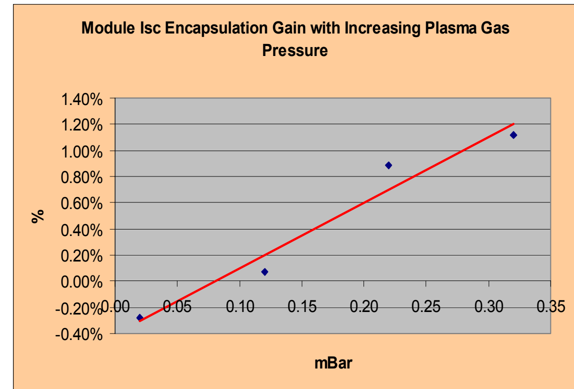

Figure 5 Encapsulated I_{SC} improved by plasma gas pressure

These improved encapsulated cell efficiencies are now available in BP Solar modules typified by the BP3160 product (Figure 6) at 160 Watts nominal, with 5% tolerance on maximum power and good process distribution. With a 25-year power warranty, BP Solar Silicon Nitride modules have achieved IEC61215 certification and are manufactured in ISO9001 accredited facilities.

Figure 6 BP3160 Solar Array

4. REFERENCES

[1] S. Roth, *Proc. 12th Workshop on Crystalline Silicon Solar Cell Materials and Processes* (NREL, 2002), p. 163

[2] Box, Hunter, *Statistics for experimenters*

[3] W. A. Langford, M. J. Rand, "The hydrogen content of plasma deposited silicon nitride", Journal of Applied Physics, **49**, No 4, pp. 2473-2477, April 1978